TEMPLATE SYNTHESIS OF POLY(N-METHYLPYRROLE) & POLYPYRROLE BASED SUPERCAPACITOR: FABRICATION AND CHARACTERIZATION

by

CANAN BARIŞTIRAN

Submitted to the Graduate School of Engineering and Natural Sciences
in partial fulfillment of the requirements for the degree of
Master of Science

Sabanci University

Spring 2007

APPROVED BY:

Prof. Dr. Yuda Yürüm .....

Assoc. Prof. Dr. Yusuf Menceloğlu .....

Prof. Dr. Atilla Güngör .....

Assoc. Prof. Dr. Yaşar Gürbüz .....

Asst. Dr. Melih Papila .....

DATE APPROVAL: .....

TEMPLATE SYNTHESIS OF POLY(N-METHYLPYRROLE) & POLYPYRROLE BASED SUPERCAPACITOR: FABRICATION AND CHARACTERIZATION

Canan BARIŞTIRAN

Material Science and Engineering, MSc Thesis, 2007

Thesis Supervisior: Prof. Dr. Yuda YÜRÜM

Keywords: conducting polymer, electrochemistry, supercapacitor

Abstract

This study can be categorized into two parts. The first part aims to obtain nano-sized, new promising active electrode materials for supercapacitor application by using commercially available monomer. The polymer of N-methylpyrrole was studied to obtain nano-size form by applying a template synthesis method. Its morphology characterization was performed by scanning electron microscopy (SEM). To enhance the electrical conductivity of the obtained polymer, template synthesized poly(N-methylpyrrole) with gold nano particle was combined. The resulted polymer/gold material has been characterized by SEM techniques.

The second aim was to build a polypyrrole based solid state supercapacitor prototype by using proton polymeric electrolytes having the common acids of H_3PO_4. The effect of the duration of polymerization on electrode materials for supercapacitor devices was also studied. The performance characteristics of fabricated supercapacitors were evaluated by ac. electrochemical impedance spectroscopy, cyclic voltammetry techniques and the study of surface morphology of the active electrodes were performed by scanning electron microscopy.

POLİ (N-METİLPİROL)'ÜN ŞABLON SENTEZİ & POLİPİROL TABANLI SÜPERKAPASİTÖR: ÜRETİMİ VE KARAKTERİZASYONU

Canan BARIŞTIRAN

Malzeme Bilimi ve Mühendisliği, Yüksek Lisans Tezi, 2007

Tez Danışmanı: Prof. Dr. Yuda YÜRÜM

Anahtar kelimeler: iletken polimer, elektro kimya, süperkapasitör

Özet

Bu çalışma iki bölümden oluşmaktadır. Birinci bölümde, süperkapasitör uygulamalarında kullanılmak üzere yeni, aktif malzemelerin nano boyuttaki sentezi, ticari olarak elde edilebilen monomerler kullanılarak gerçekleştirilmiştir. N-metilpirol monomeri kullanılarak elde edilen polimerin nano boyuttaki sentezi, şablon sentez yöntemi kulllanılarak gerçekleştirilmiştir. Elde edilen malzemenin yüzeysel karakterizasyonu taramalı elektron mikroskopuyla gerçekleştirilmiştir. Ayrıca, Poli(N-metilpirol)'ün elektriksel iletkenliğini arttırmaya yönelik olarak, altın nano boyuttaki parçacıklarla birleştirme çalışmaları yapılmış, sonuçlanan polimer/altın nano parçacık yapısının karakterizasyonu taramalı elektron mikroskopi yöntemiyle yapılmıştır.

İkinci bölümde, laboratuar ortamında çalışan süperkapasitör prototipi yapmak amaçlanmıştır. Yapılandırılan süperkapasitörlerde aktif elektrot malzemesi olarak, monomeri ticari olarak elde edilebilen polipirol, elektrolit ayıraç olarak proton polimerik elektrolit kullanılmıştır. Hazırlanan elektrotlar için farklı polimerleşme süreleri kullanılarak, cihazlardaki kapasitans performansına etkisi incelenmiştir. Gerçekleştirilen süperkapasitör prototiplerinin performansları elektrokimyasal impedans spektroskopi ve dönüşümlü voltametre teknikleri kullanılarak ölçülmüştür. Ayrıca, elektrotların yüzeysel özelliklerini incelemek amacıyla, taramalı elektron mikroskopundan yararlanılmıştır.

ACKNOWLEDGEMENTS

First and foremost, I gratefully thank to my beloved adviser Gürsel Sönmez for his support and creation of this thesis. Even we could not complete this work together, I tried to do my best as I learned from him.

I would like to express my special thanks to Prof. Dr. Yuda Yürüm for guidience and supporting during all steps involved in the research for this thesis. It was not possible to finish this work without his help.

I would also like to thank to Assoc. Prof. Yusuf Menceloğlu for his invaluable contribution throughout my graduate studies.

In addition, I want to thank my colleagues and friends especially İbrahim İnanç, Aslı Nalbant, Ozlem Sezerman, Burcu Saner, Cenk Gümeci, Murat Giray, Ayça Erden, Arzu Ergintav, Onur Esame for their support and friendship.

Finally, I would like to express my deepest thanks to my family and Mehmet for everything throughout my life.

Table of Contents

List of Figures

List of Tables

Canım Babam'a…

1

Chapter 1

INTRODUCTION

1.1 Motivation and Research Goals

It has been already known that electrical energy can be stored in batteries or in capacitors for years. On the other hand, renewable energy sources are needed because of the excess consumption of the fossil fuel sources, recently [1, 2]. Supercapacitor, which is also called electrochemical capacitor or ultracapacitor, is a new trend as an alternative energy storage device. Mainly, the working mechanism of supercapacitor relies on the separation of the ions at the interface between electrode and electrolyte. Therefore it is also called electrochemical double layer capacitor [3].

Energy density and power density of electrochemical capacitors reside between batteries and capacitors [4]. The Ragone chart is illustrated in Figure 1-1, to compare the energy and power density of electrochemical capacitor and battery characteristics. This chart is used for performance comparison of various energy storing devices.

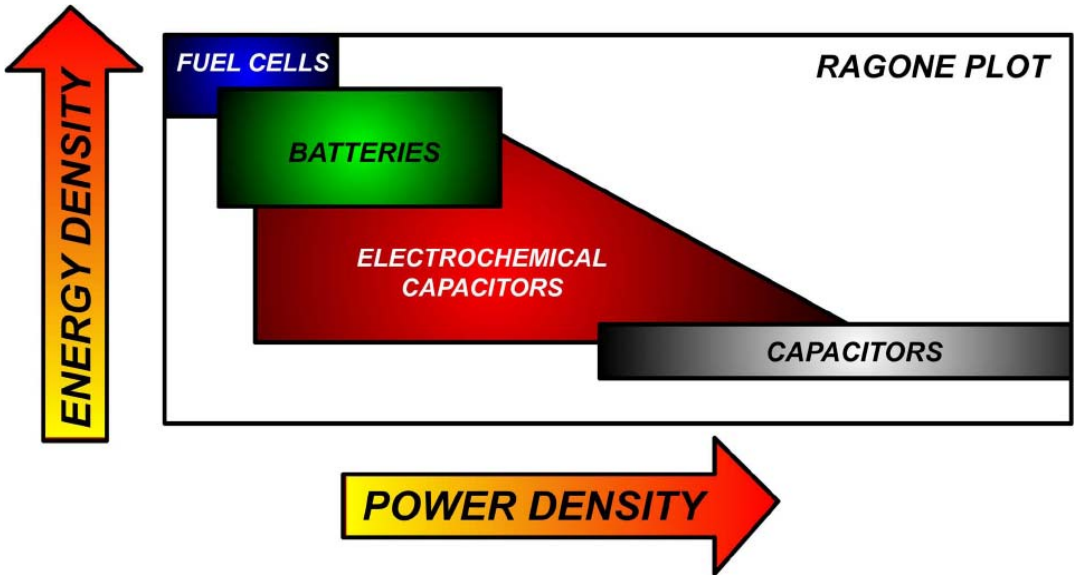

Figure 1-1 Ragone plot

As seen from the Ragone plot, supercapacitor plays a bridge role between those of batteries and conventional capacitors. With this promising property, they are mainly utilized for power backup for electronic circuits [5]. These capacitors are also good candidates as load leveling applications in electric vehicles as well as pulse power applications [6, 7].

Supercapacitor devices are fabricated using two electrodes, which allow a potential across the electrode material, and a separator for preventing short contact between the electrodes. Since there are two electrodes, there are also two double-layers on each electrode-electrolyte interface. These two double layers are connected as series in an electrochemical capacitor device. The electrodes are selected among the high surface area materials such as porous carbon materials, in order to maximize the surface area of the double layer. Therefore, high energy density in supercapacitor is possible due to the high electrode-electrolyte interface surface area and a small charge layer separation [8, 9].

Taking the advantage of the use of large surface area electrode materials in supercapacitors, carbon based capacitors have been gaining attention due to their low cost, extremely high cycle life, and wide range of operating temperatures [10].

However, scientists tend to construct electrochemical capacitors using conducting polymers in order to provide much more energy and power densities than carbon based capacitors, since conducting materials give rise to additional capacitance with the reaction of redox [11, 12]. In addition, they are less expensive, easier to realize in the form of thin films and can store charge in all regions of their volume [13].

The aim of this study can be categorized into two parts. For the first part of this study, it was aimed to obtain new promising active electrode materials for supercapacitor in nano-size by using commercially available monomer. The polymer of N-Methyl pyrrole was studied to obtain in nano-size form by applying a template synthesis method. Its morphology characterization was performed by scanning electron microscopy (SEM). To enhance the electrical conductivity of the obtained polymer, it was tried to combine template synthesized poly(N-methylpyrrole) with gold nano particle. The resulted polymer/gold material was characterized by SEM techniques.

For the second part, the aim was that to build polypyrrole based solid state supercapacitors by using proton polymeric electrolytes having the common acids of H_3PO_4. The effect of duration of polymerization on electrode materials for supercapacitor devices was studied. The performance characteristics of fabricated supercapacitors by using these electrode materials were evaluated by ac. impedance spectroscopy, cyclic voltammetry techniques and the study of surface morphology of active electrodes was performed by scanning electron microscopy. It was expected that high specific capacitance is possible for the supercapacitor which has active electrode materials prepared by applying longest duration of polymerization.

1.2 Theory of Supercapacitors

The fundamental physical processes that take place in an electrochemical capacitor will be addressed in this part to simulate the working mechanism properly. It starts with the basics of capacitors and continues with the storage mechanisms of the specified types of capacitors.

Since the working principle of the electrochemical capacitors is similar to the conventional ones, reviewing conventional capacitors could be a good start.

Conventional capacitors consist of two conducting materials separated by a dielectric as shown in Figure 1-2. The charge accumulations on the conducting plates are achieved by applying an electrical potential to the conductors. The conductor plates remain at their charged state until they are brought into contact, when the applied potential is removed.

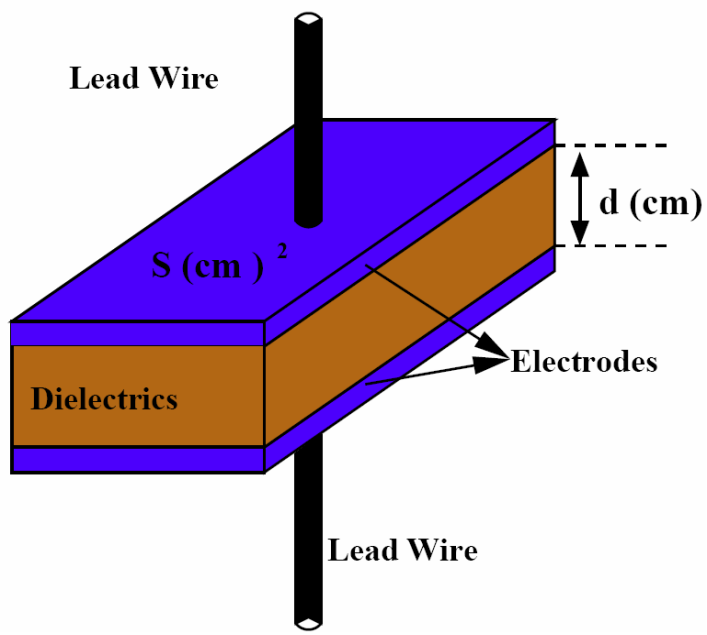

Figure 1-2 Conventional electrostatic capacitor structure

The capacitance is defined as the amount of charge which can be stored charge for an applied voltage and expressed as in equation (1.1).

$$C = \frac{Q}{V} = \varepsilon \frac{A}{d} \qquad \textbf{(1.1)}$$

The electrostatic energy stored in a conventional capacitor is given in equation (1.2).

$$U = \frac{1}{2}CV^2 = \frac{1}{2}QV \qquad \textbf{(1.2)}$$

where C is the capacitance in Farads, Q is the charge in Coulombs, V is the electrical potential in Volts, ε is the dielectric constant of the dielectric, A is the surface area of conductor plate, d is the thickness of dielectric, and U is the electrical potential energy [14].

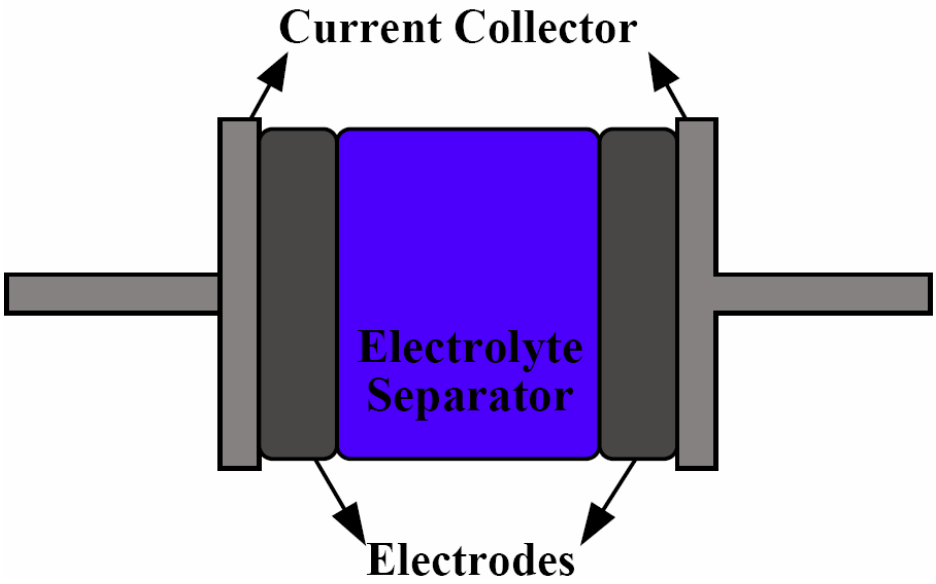

Figure 1-3 Conceptual electrochemical capacitor structure

Although electrochemical capacitors have similar working principle as the electrostatic conventional capacitors, the charge accumulation in electrochemical capacitor does not occur on the conducting plates which are separated by an insulator, in contrast to conventional capacitors. The conceptual structure of electrochemical capacitors is illustrated in Figure 1-3. In electrochemical capacitors the charge accumulation is achieved at the interface between the electrolytic solution and the electrode surface in electrochemical capacitors as shown in Figure 1-4 [15]. At this point, it should be noticed that the reason for referring to electrochemical supercapacitors as double layer capacitor is the fact that the accumulated charge occurs on the electric double layer [16]. The ionic separation distance in electrochemical capacitor depends on the size of the ions which is typically in the

order of 5 to 10 angstroms and on the concentration of the electrolyte. Therefore, supercapacitors which depend on the principle of electrochemical double-layer capacitance exhibit a specific capacitance which has a greater magnitude than that of electrostatic capacitors.

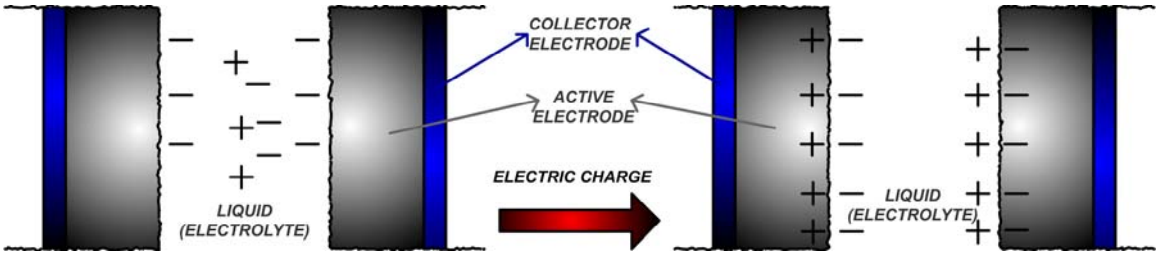

Figure 1-4 Electrochemical charge storage mechanism

The accumulated specific capacitance in the electric double layer formed at the interface between the electrode material and the electrolyte solution is expressed in equation (1.3) which is proposed by the Helmholtz in 1879.

$$\frac{C}{A} = \frac{\varepsilon}{4\pi\delta} \tag{1.3}$$

Where C is the capacitance, A is the surface area of the electrode material, ε is the dielectric constant of the electrolyte solution, δ is the distance (from the electrode to the center of the ion).

1.2.1 Storage mechanism of Supercapacitors

As discussed in the previous part, in electrical double layer capacitor, charge accumulation is achieved electrostatically, but some additional capacitance is also possible by the reactions that can happen on the surface of the electrode material. This extra capacitance is called as pseudo-capacitance [17]. The reactions, which facilitate pseudo-capacitance, depend on applied electrical potential and therefore show capacitive behavior [18]. In the following part, double layer capacitance and pseudo-capacitance behaviors have been discussed separately.

1.2.1.1 Electrical Double Layer Capacitor

The storage mechanism of the electrical double layer capacitor relies on the separation of electronic and ionic charges at the interface between the electrode materials and the electrolyte solution. It is electrostatic, principally [19, 20]. It has been developed some models in order to understand electrical processes which occur at the interface between the electric conductor and the electrolyte solution.

The earliest investigation, in which two charged mono-layers considered, was done by Helmholtz in 1879. This model assumes charged electrode forms one layer and the ions in the electrolytic solution form the other layer as shown in Figure 1-5. The capacitance equation of Helmholtz model is given in equation (1.3). This model failed to account for the electrolyte concentration and it neglects interactions occurring further from the electrode than the first layer of adsorbed species.

After investigation of Helmholtz's model, some improvements in which diffusion phenomenon of electrical double layer considered were done by Gouy and Chapman in 1913. This model considered the thermal motion of the ions and the electrolyte concentration both influencing the value of the double layer capacity. The double layer would not be as compact as in the Helmholtz description, but of variable thickness and the ions being free to move as shown in Figure 1-6 conceptually.

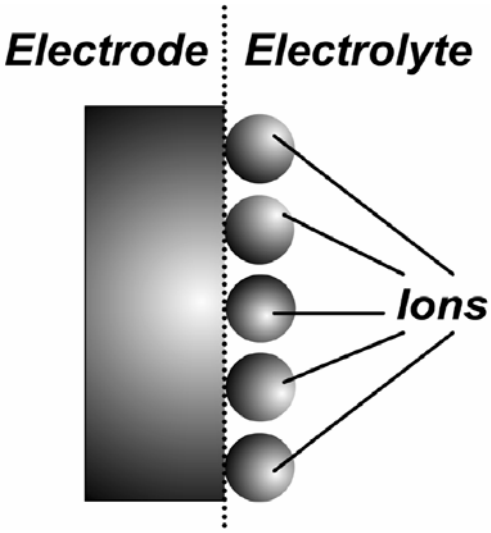

Figure 1-5 Helmholtz double layer model

The recent electrical double layer model is improved by Stern and called as Gouy-Chapmen-Stern model which is a combination of Gouy-Chapmen diffuse model and Helmholtz's model. In this model, it is considered that ions have a finite size and that the charge is located in the center. The double layer was divided into two parts, a compact layer of ions next to the electrode followed by a diffuse layer extending into bulk solution as shown in Figure 1-7. As seen from the figure, the closest approach of the diffuse ions to the electrode surface called the outer Helmholtz plane, while the layer of specifically adsorbed ions at the electrode surface as being the inner Helmholtz plane [21].

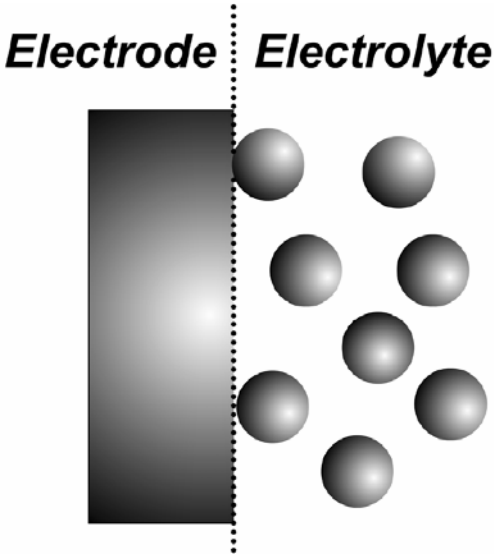

Figure 1-6 Gouy-Chapman diffuse model

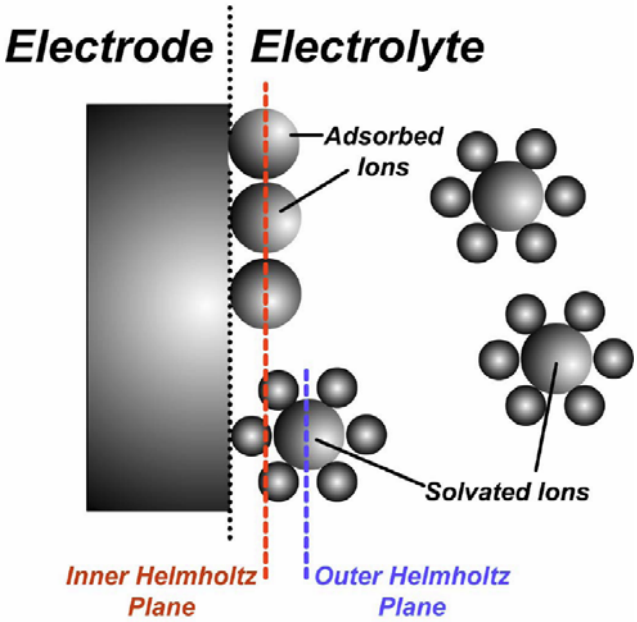

Figure 1-7 Gouy-Chapman-Stern model

1.2.1.2 Pseudo-capacitance

As a contribution to the capacitance that arises from the separation of charge in the double-layer, additional capacitance can be produced from the reactions that occur on the surface of the electrode [22]. The amount of charge required to realize these reactions depends on the potential, resulting in a phenomenon which is called as 'pseudo-capacitance'. The pseudo-capacitance occurs on the electrode materials as a result of the reactions and denoted as ''pseudo'' in order to differentiate it from electrostatic capacitance. Pseudo-capacitive behavior arises from the redox reactions or adsorption of ions by the electrode surface [23]. Due to the fundamental differences between these two types of reaction processes, their detailed information is discussed in the following part.

1.2.1.3 Redox

The redox reactions which are fast and reversible, take place on the electrode materials at characteristic potentials as in batteries, and give rise to what is called pseudo-capacitance. Redox reaction which has pseudo-capacitive effect comes out through the surface functionalities at the electrode surface contribute to the charge storage of supercapacitor devices. The pseudo-capacitance due to the redox reactions

is 10 times larger than the pseudo-capacitance which comes from adsorption and 100 times larger than the double layer capacitance which is electrostatic [24].

In a redox reaction involving an oxidant and a reductant in the form of "oxidant + ze^- → reductant", the potential, E, is given by the Nernst equation as shown in equation (1.4).

$$E = E^0 + \frac{RT}{zF} \ln \frac{\Re}{1 - \Re} \tag{1.4}$$

where E^0 is the standard potential, R is the gas constant, T is the absolute temperature, F is the Faraday constant, and $\Re$ is defined as [ox]/([ox]+[red]), (square brackets mean concentrations of species).

As mentioned in the previous part, the capacitance is defined as the amount of charge which can be stored charge for an applied voltage. Therefore, differentiation of equation (1.4) generates a pseudo-capacitive relation due to the fact that the amount of charge q (given by the product zF) is a function of the potential E [25, 26].

1.2.1.4 Adsorption of ions

Adsorption of the ions in order to arise a mono-layer on the electrode surface which is a reversible process, outcomes in a faradaic charge transfer, and therefore gives arise to pseudo-capacitance in a similar style with redox reactions. The adsorption and desorption process can be demonstrated as in chemical equation (1.5),

$$A_c^{\pm} + S_{1-\Theta_A} \pm e_V^- \leftrightarrow S_{\Theta_A} A_{ads} \tag{1.5}$$

where A is the ionic species, S is the substrate, c is the concentration of depositable ions, $1\text{-}\theta_A$ is the partial free surface area accessible for adsorption, and V is the electrode potential [27].

As shown in the equation (1.5), when the characteristic electrical potential is applied to the electrode, electron transfer takes place on the electrode material and it gives rise to adsorption of corresponding ion species in the electrolyte onto the electrode material. These adsorbed ions on the electrode material consists a mono-layer on the electrode material and contribute to forming of double-layer so that causes an extra capacitive behavior on each electrode.

To sum up of scientific charge storage mechanism background about supercapacitor, high values of specific capacitance are attainable through electrochemical double layer technology and often pseudo-capacitance. Double-layer capacitance offers good charge storage capabilities due to possessing high surface-area materials as electrodes, and the fact that charge separation occurs at atomic dimensions. Pseudo-capacitance that comes out from redox or ion sorption reactions further improves the achievable capacitance.

1.2.2 Performance principles of supercapacitors

In order to apply the supercapacitors to various practical devices, even to electric vehicles, the development of supercapacitors with both high power density and high energy density is necessary. The maximum power density of a supercapacitor is given by (1.6),

$$P_{\max} = \frac{V^2}{4.ESR} \qquad \textbf{(1.6)}$$

where V is the initial voltage, and ESR is the equivalent series resistance [28]. Therefore, the significant factors determining the power of supercapacitors are the resistance of the electrode itself, the resistance of the electrolyte within the porous layer of the electrode, and the contact resistance between the electrode and the current collector [29].

The maximum storage energy, based on the electrode mass is given by equation (1.7)

$$E = \frac{1}{8} C_P V^2 \qquad \textbf{(1.7)}$$

where *Cp* is the specific capacitance of the material. Therefore maximizing the capacitance of the electrode is the key factor to increasing the energy density [30].

Electrochemical capacitors are close cousins to batteries. The simple circuit shown in Figure 1-8 illustrates the small-signal model of capacitor.

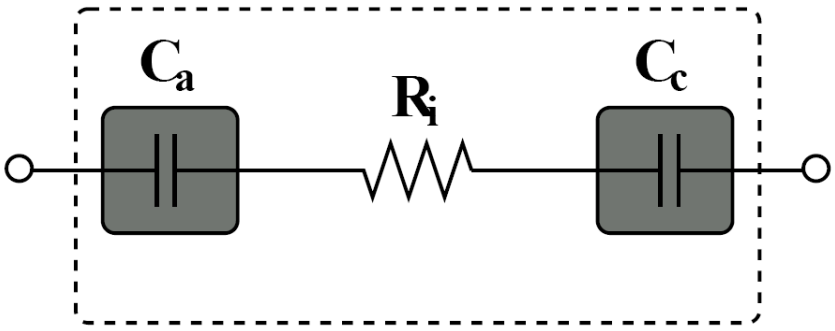

Figure 1-8 Simple circuit schematic for supercapacitor

Here, C_a and C_c are the double-layer capacitances of the anode and cathode, respectively. R_i is the internal resistance of the cell. Since the capacitors are in series the total capacitance value is $\frac{1}{C} = \frac{1}{C_a} + \frac{1}{C_c}$ [27, 31].

If Ca = Cc, as would be expected for a supercapacitor, then the total capacitance is expected to be the half of the anode or the cathode capacitors ($C = \frac{1}{2} \times C_a$) [32].

Chapter 2

2

EXPERIMENTAL

2.1 Materials

The chemicals of N-Methylpyrrole, pyrrole, lithium perchlorate ($LiClO_4$) (Aldrich Chemical Co.); chloroform, methanol, propylene carbonate (Merck Chemical Co.); poly(vinyl alcohol), (PVA, $M_W \approx$ 72 000, Merck Chemical Co.); poly(ethylene oxide), (PEO, $M_W \approx$ 400 000, Aldrich Chemical Co.); polyethylene glycol (PEG, $M_W \approx$ 4000, Merck Chemical Co.); phosphoric acid, (H_3PO_4, Aldrich Chemical Co.), sodium lauryl sulfate (Henkel Chemical Co.) were used as received. Polycarbonate membrane filter (pore size ca. 220 nm) from Millipore was used as template. Gold nano-particles were synthesized by Asst. Prof. Cleva Ow-Yang's study group in Sabanci University/ Material Science & Eng. Programme.

Indium-tin oxide coated conducting glass (ITO, 7 mm X 50 mm X 0.7 mm, sheet resistance: 5-15 Ω per square) from Delta Technologies was used as working electrodes. Platinum wire (99,9 %) and silver wire (99,9 %) electrodes were used as counter electrode and reference electrode respectively.

2.2 Template synthesis of Poly(N-methylpyrrole)

Polycarbonate membrane filter was utilized as a template to realize nano-arrays of Poly(N-methylpyrrole). Polycarbonate membrane has an average pore size of ca 220 nm as shown in SEM image in Figure 2-1.

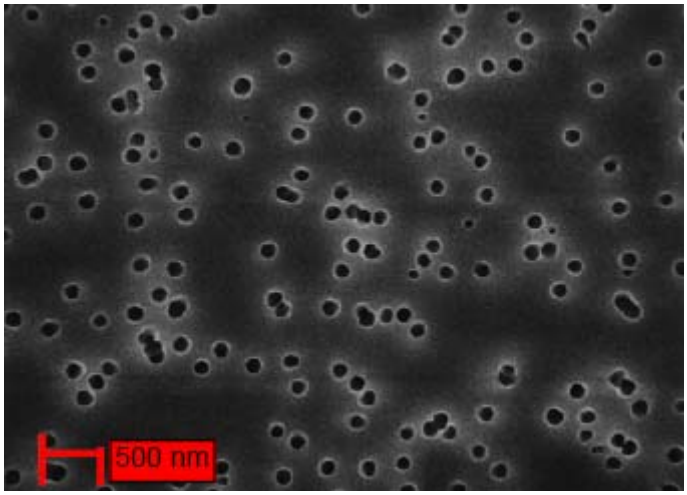

Figure 2-1 SEM image of Polycarbonate membrane

For template synthesis of Poly(N-methylpyrrole), polycarbonate membrane was sandwiched between the two compartments of a U-shaped glass tube which is illustrated in Figure 2-2. As seen from the figure, the monomer and the oxidant solution were separated with the membrane in which the solutions diffused through each other by the way of the pores of polycarbonate membrane.

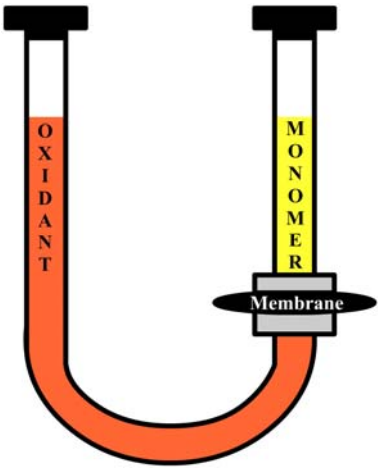

Figure 2-2 Experimental setup U-tube for polymerization

Poly(N-methylpyrrole) nano-arrays were achieved using an aqueous N-methylpyrrole (0,05 M) solution and an iron (III) chloride (0,20 M) oxidant solution in water. Sodium lauryl sulfate was also added to the monomer solution as surfactant to decrease surface tension. The aqueous monomer solution in the shorter part of the U-shaped glass tube and the aqueous solution in the longer part were separated with the polycarbonate membrane filter. As soon as the monomer and the oxidant solutions contact with each other, the reaction starts by diffusing through the pores of the membrane filter. After 3 hours of successive polymerization time, polycarbonate membrane was taken out by removing two separate parts of the U-tube and washed with methanol and double-distilled water, respectively. Then, polycarbonate membrane was dissolved with chloroform and templated Poly(N-methylpyrrole) nano arrays remained.

Once the polymerization was completed, the aqueous solution of gold nano-particles was passed through the membrane by applying vacuum in order to deposit the gold nano-particles on to Poly(N-methylpyrrole) nano arrays. After this application, the membrane was dissolved with chloroform and the resulting structure was characterized by scanning electron microscopy technique.

2.3 Fabrication of devices

The prototype of fabricated supercapacitor is presented in Figure 2-3. It was consisted of two thin and the same polymer films deposited on conducting glass ITO (indium tin oxide) electrodes and separated by a polymer electrolyte [33].

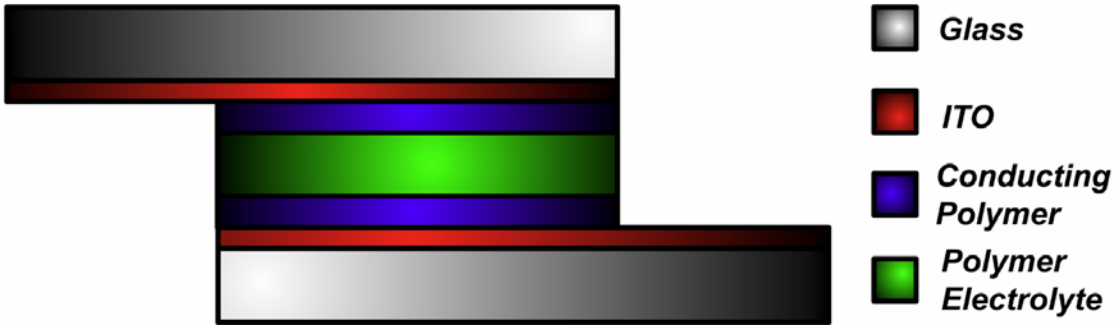

Figure 2-3 Redox Supercapacitor Configuration

In the following parts, experimental preparation information for electrodes and electrolyte has been shown.

2.3.1 Electrode preparation and characterization

Electrochemical polymerization process was carried out in a single compartment electrochemical cell by implementing a standard three electrodes configuration. The electrochemical bath contained of monomer and supporting electrolyte dissolved in suitable solvent. A general set-up for electrochemical polymerization cell is given in Figure 2-4.

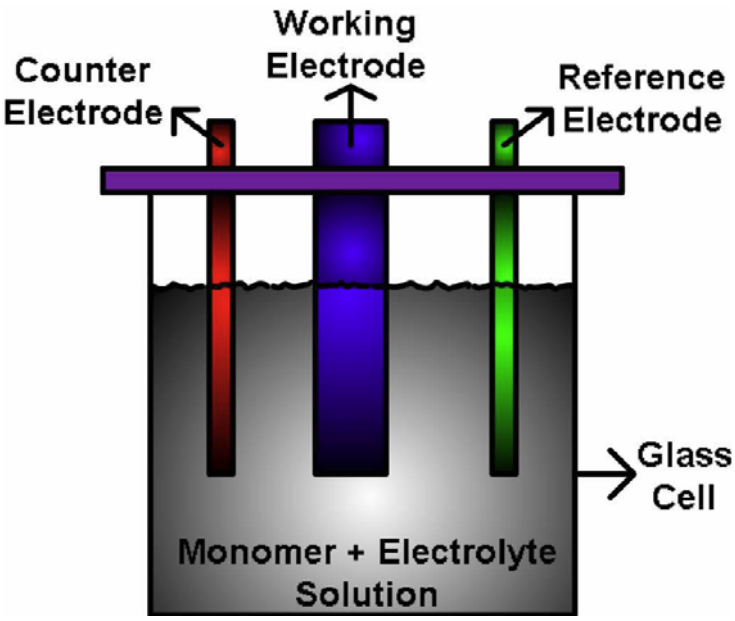

Figure 2-4 Electrochemical polymerization cell set-up

In this work, a platinum wire and silver wire were used for the counter and reference electrodes, respectively. ITO coated glass slides were utilized as the working electrode. The polypyrrole was deposited directly on ITO substrates electrochemically. These experiments were performed using Epsilon EC potentiostat / Galvanostat and the supporting electrolyte and the solvent used during electropolymerization were $LiClO_4$ (lithium perchlorate) and propylene carbonate respectively.

The electro-syntheses steps were carried out in a one-compartment, three electrode cell contains 0,1 M pyrrole and 0,2 M $LiClO_4$ solutions in propylenecarbonate. The electro-depositions on ITO was performed with a constant current of 2 mA for different duration of times such as 1 minute, 5 minute and 10 minute. The deposition area was taken as 0,7 cm^2 on the working electrode and this area was used for all test structures to improve the reliability of the measurements.

The schematic cross-section of the polymerized working electrodes mentioned above is illustrated in Figure 2-5.

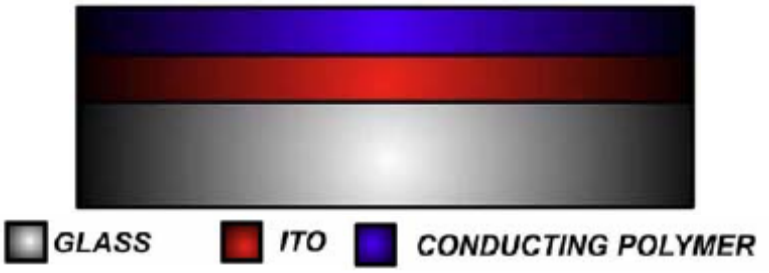

Figure 2-5 Cross-Section of the Polymerized working electrode

Scanning electron microscopy was used for the surface morphology characterization of the prepared electrode to construct supercapacitor.

2.3.2 Preparation of polymer electrolyte

Polymer electrolytes are used as a separator for preventing the short contact between the two electrodes of supercapacitor [34]. In this study, poly (vinyl alcohol) (PVA)-H_3PO_4 was used as proton conducting polymer electrolyte.

The composition for the proton conducting polymer electrolyte blend was chosen as 60:40 (w/w) of PVA: H_3PO_4. First of all, the PVA-H_3PO_4 blend was prepared by dissolving the appropriate amount of PVA in double-distilled water at 85 °C. Secondly, H_3PO_4 (40% w/w) was added after consequent cooling of the PVA solution. Then the mixture was stirred for 12 hours and lastly poured into a Teflon mould. To obtain the film form of the polymer electrolyte, it was waited for 12 hour

for the room temperature evaporation of the solvent. At the end, the resulted polymer electrolyte of PVA-H_3PO_4 film thickness was measured using Dektak surface profiler. The bulk electrical conductivity of the polymer electrolyte film was evaluated by Gamry® complex impedance spectra under the room temperature condition.

2.3.3 Supercapacitor device construction and characterization

The entire electrode sets and polymer electrolyte film, which were described previously, were used for the construction of supercapacitor devices. The proton conducting polymer electrolyte was used between two electrode materials as a seperator. Three different models of capacitor cells were designed symmetrically and detailed in Table 2-1,

Table 2-1 Fabricated Different models of Supercapacitors

Type of Device	**Electrolyte Separator**	**Electrode Type**	**Duration of Deposition**
Type A	PVA-H_3PO_4	Ppy	1 min
Type B	PVA-H_3PO_4	Ppy	5 min
Type C	PVA-H_3PO_4	Ppy	10 min

where “Ppy” signify polypyrrole, as the active electrode materials.

The performance of the constructed supercapacitors was characterised by a.c. electrochemical impedance spectroscopy (Gamry®), cyclic voltammetry (Epsilon® potentiostat/galvanostat). For the characterization method of cyclic voltammetry, measurement setup, which has three electrode systems originally, was reduced to a two electrode system by attaching the reference and the counter electrodes together. All the cyclic voltammeter experiments were done at different scan rates (10-50-100 mV/s) for a floating potential between -0.95 V and 0.95 V. This potential difference was applied with respect to the Ag wire reference electrode. AC impedance measurements were carried out in the frequency range 10 mHz to 100 kHz.

3

Chapter 3

RESULTS AND DISCUSSION

3.1 Characterization results of templated Poly (N-methylpyrrole)

Polymerization using a specific template is a powerful technique since it has the ability to control the dimensions and shapes of the polymers obtained. The outside diameter of the polymer is determined by the diameter of the pores in the template, and the length of the polymer is determined by the thickness of the template. It is, however, more difficult to control the inside diameter or, correspondingly, the wall thickness of template-synthesized polymers.

As it is explained in the experimental part, for the template polymerization, used monomer and chemical oxidant were N-Methylpyrrole and $FeCl_3$, respectively. When these chemicals contact each other, the polymerization mechanism starts with the electron transfer from N-methylpyrrole to $FeCl_3$ and continuous with electron transfer between the monomer or the growing chain and the chemical oxidant. The benefit of this type of polymerization is that it can be used to produce large quantities of material when compared to electrochemical synthesizing of polymer techniques.

SEM was utilized in order to determine the final morphology of the polymer and the gold nano-particle combined polymer. The inner diameter is an important factor for supercapacitors since as the surface area increases, the active layer of

supercapacitor's capacitance increases as well. By the use of SEM, we determined the both inner and outer diameter of the fibers.

In the case of structural behavior, depending on the membrane, the shapes of cylindrical nanostructures were obtained as seen from all the SEM figures. Figure 3-1 indicates a typical bunch of fibers of Poly(N-Methylpyrrole) having 217 nm outer diameter, matches the pore size value of the polycarbonate template. As seen from Figure 3-1, some fibers have an inner diameter while some fibers are completely full, and rely on difficulty to control the wall thickness of the polymer by using template.

Because of the electrostatic interactions between the positively charged polymer which is obtained and the anionic sites on the pore walls of the membrane, the alignment of fibers has been completed in the length of 17,56 μm, illustrated in Figure 3-2. This value for the length of obtained fibers is very near to the 20 μm thickness value of the membrane.

By the use of the surfactant in the medium of polymerization, smooth and continuous surface on the fibers have been achieved as illustrated in Figure 3-3.

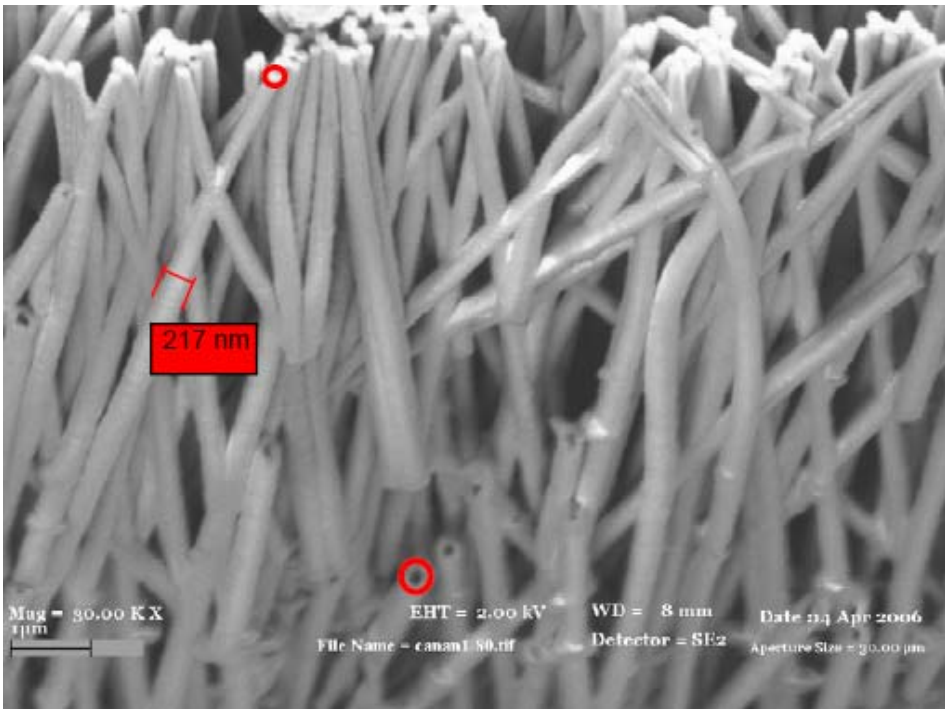

Figure 3-1 SEM image of templated Poly(N-methylpyrrole)

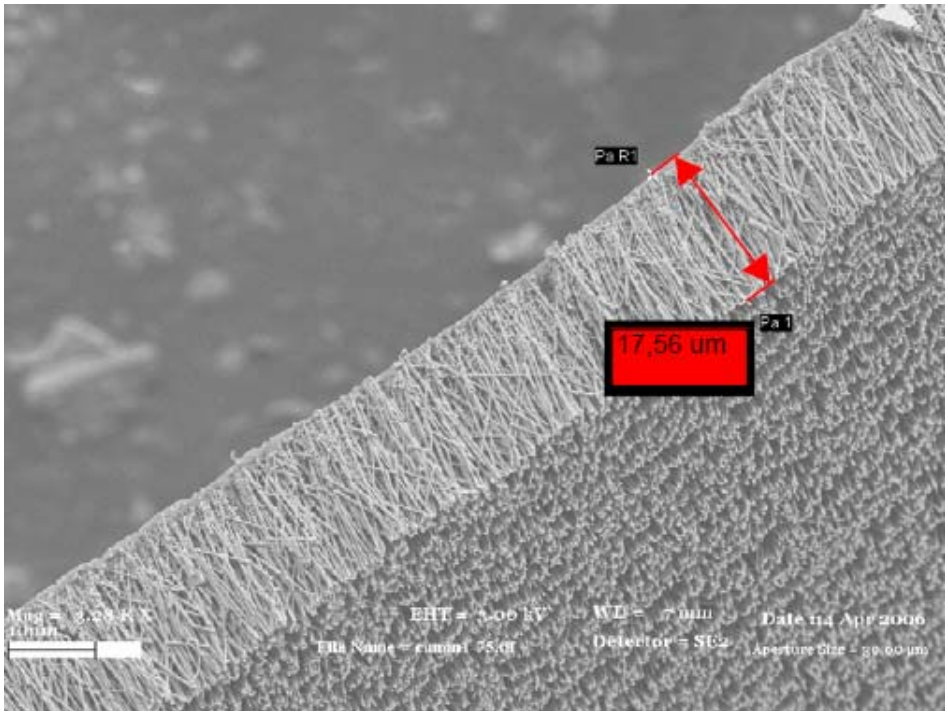

Figure 3-2 SEM image of templated Poly(N-methylpyrrole)

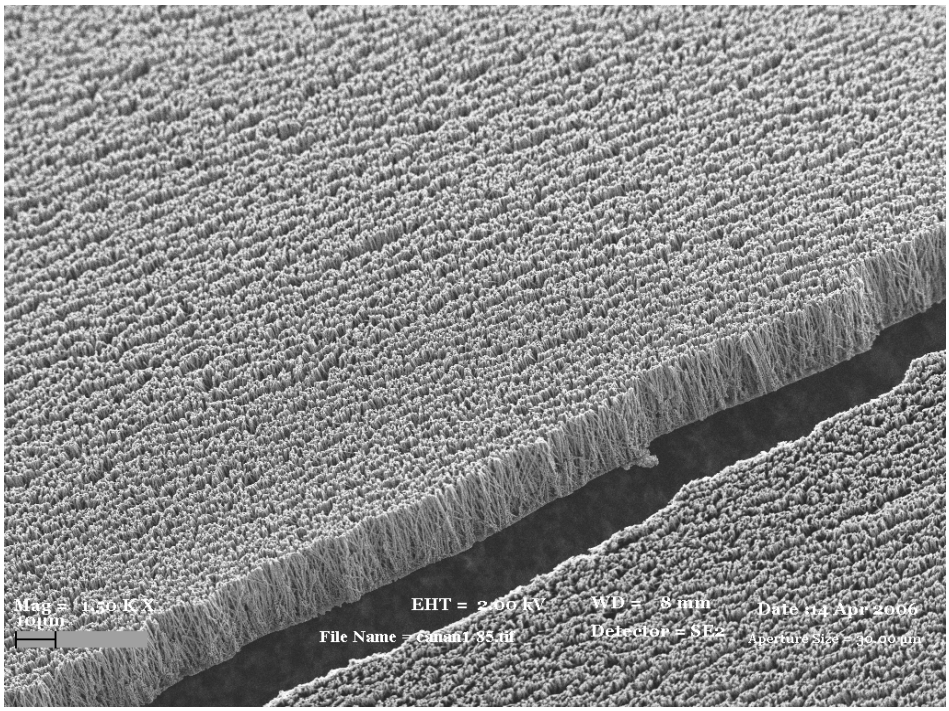

Figure 3-3 SEM image of templated Poly(N-methylpyrrole)

SEM images of gold nano-particle combined Poly(N-methylpyrrole) fibers have been shown in Figure 3-4. As seen from the figure, by the effect of the vacuum to deposit gold nano-particles on the templated polymer is that, all the polymer fibers have an obvious inner diameter of 179.5 nm.

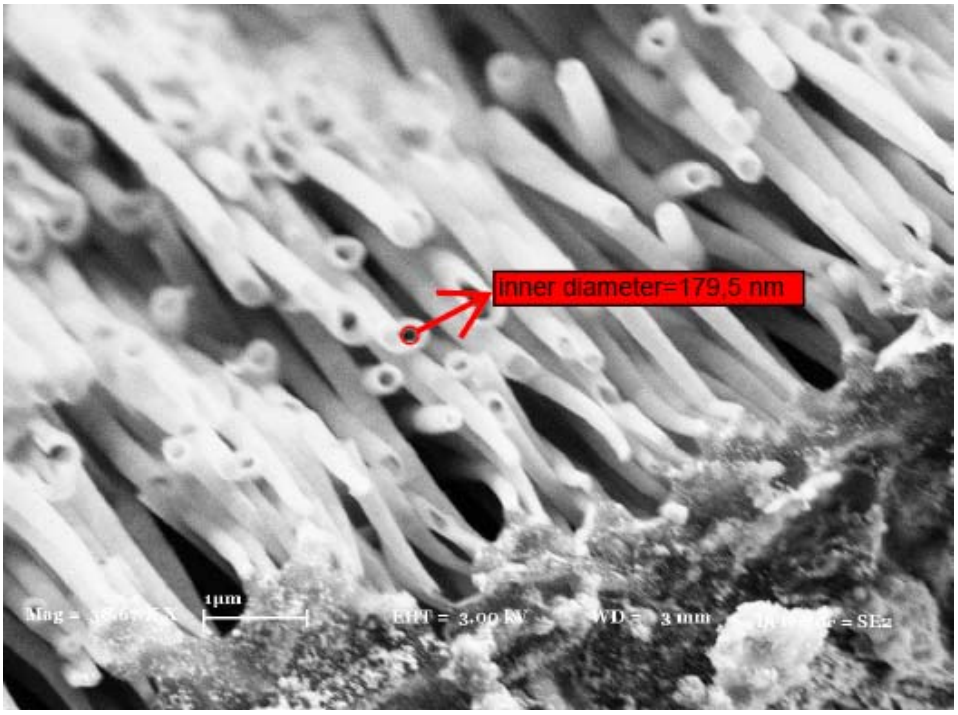

Figure 3-4 SEM image of gold nano-particle /templated Poly(N-methylpyrrole)

Figure 3-5 demonstrates that the combination of gold nano-particle and fibers of polymer has been obtained, especially at the bottom layer of the fibers. When the magnification was increased as much as 500.00 KX, in the area which has gold nanoparticles, the gold nano particles have a diameter of 15 nm, as anticipated.

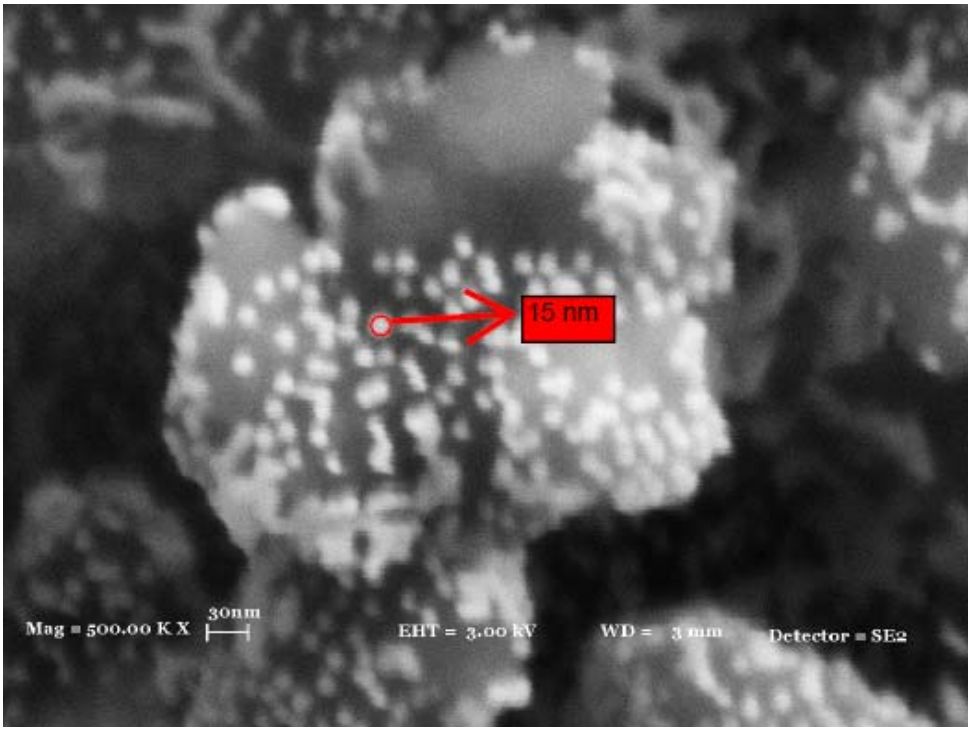

Figure 3-5 SEM image of gold nano-particles on templated Poly(N-methylpyrrole)

3.2 Characterization results of devices and their components

3.2.1 Characterization of electrodes

Conducting polymer is preferred as an active electrode material to fabricate the supercapacitors in this work since it is promising material due to the fact that the charge is accumulated in the bulk of the polymer, the charging and discharging process is fast throughout a delocalized electronic structure, and it can be produced at cheaper prices when compared to the other alternative electrode materials (e.g. some metal oxides [35, 36] and activated carbons [37, 38]). In addition, it has high conductivity in the charged state so it is possible to obtain low equivalent series resistance in the designed device and also because of its plasticity enables its easy manufacture as a thin film [39, 40].

Also conducting polymer has the advantage of the capability of natural conductivity by modifying the chemical structure or doping process at the molecular level [41]. Generally, different techniques of making polymers conductive through composite formation (i.e. combining the polymeric materials with filler materials that are conductive such as acetylene black, metal powders, carbon black, etc.) have already been commercially utilized but there are number of negative aspects in such filled materials, for instance their conductivity depends on processing conditions, and the resulted materials may easily broken because of heavy filler.

The oxidation/reduction process of the conducting polymer can be realized electrochemically by applying the appropriate oxidizing or reducing voltage to the neutral polymer in an electrochemical cell. The charge occurred on the polymer backbone is then neutralized by a counter-ion from the electrolyte solution.

The electrochemical polymerization method was utilized to obtain polypyrrole as active electrode material. This method provides producing a conducting polymer directly on the electrode; at the same time, a fine control over the amount of deposited material and over the degree of doping. Quite advantageously, the electrochemical polymerization method offers a wide choice of 'dopant' ions which are taken from the supporting electrolyte added in the electrolyte bath. Furthermore, small amounts of material are sufficient to perform this polymerization technique. On the other hand, chemical polymerizations require substantial monomer quantities for polymerization, isolation, and characterization of the responding polymer. Extensive electrochemical studies can be performed with as little as 10-50 mg of material. Also, rapid analyses are possible in electrochemical studies which give fast information on the characteristics and properties of electro-polymerized materials.

The electro-polymerization process can be performed either potentiostatically (applying constant voltage) or galvanostatically (applying constant current) by using suitable power supplies. In this study, the galvanostatic method was preferred for electrochemical polymerization of pyrrole monomer.

The electro-polymerization process is facilitated by the fact that in many heterocycle systems, the anodically formed cation radicals quickly combine to form dimeric and higher oligomeric species and finally produce polymers as shown in Figure 3-6 [42, 43].

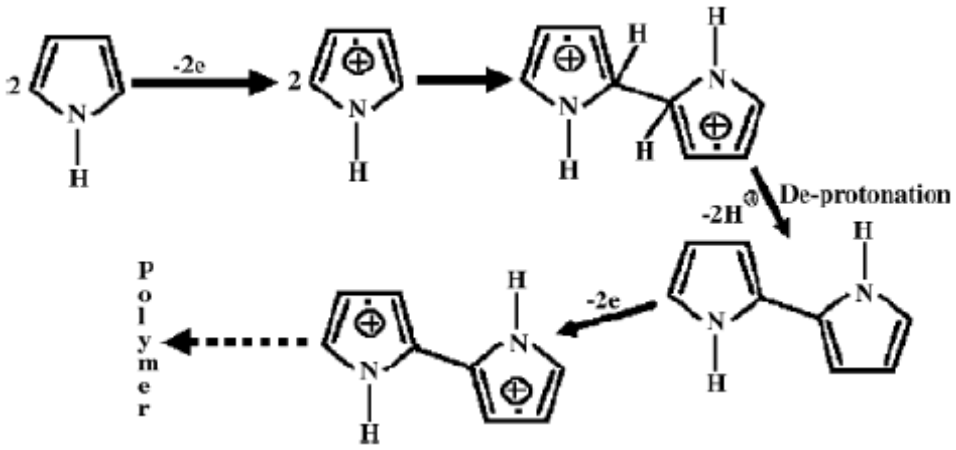

Figure 3-6 Electro-Polymerization mechanism of Polypyrrole

The minimum voltage value for successful deposition of the polymer was found as 900mV. This voltage value could be adjusted by changing the current value which flows between working electrode and reference electrode. Therefore, the monomer type enormously affects the adequate current level.

As described in section 2.3.1, a standard three electrode systems consist of a working electrode, counter electrode, and reference electrode immersed in a single dual compartment cell. The working electrode acts as a substrate for electro-deposition of polymers. Since the polymeric films are deposited by an oxidation process, it is necessary that the electrode should not oxidize concurrently with the aromatic monomer. For this reason inert electrodes Pt and ITO were used in this study.

As explained previously, fabricated supercapacitors utilized three different electrode types. Their surface morphology characterization was performed by the SEM technique. Imaging was generally operated at 2-5 keV accelerating voltage, employing the secondary electron imaging technique. The SEM image of Type-A electrode which was prepared by 1 minute duration of polymerization on ITO substrate is shown in Figure 3-7.

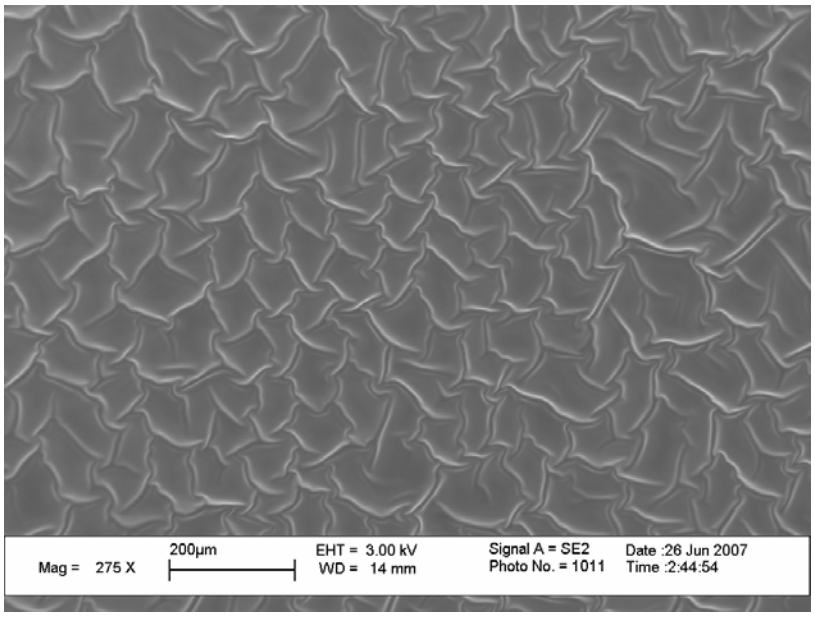

Figure 3-7 SEM image of 1 minute deposited Poly(pyrrole) on ITO electrode (electrode for Type A device)

Figure 3-8 shows a SEM image of type-B electrode which was obtained in 5 minute duration of polymerization, while Figure 3-9 depicts a type-C electrode which was prepared by a 10 minute polymerization.

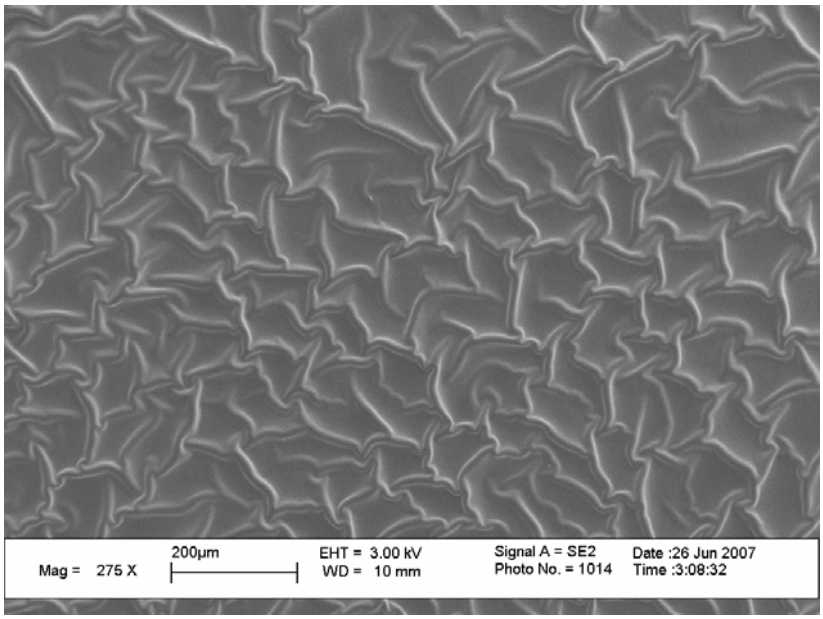

Figure 3-8 SEM image of 5 minute deposited Poly(pyrrole) on ITO electrode (electrode for Type B device)

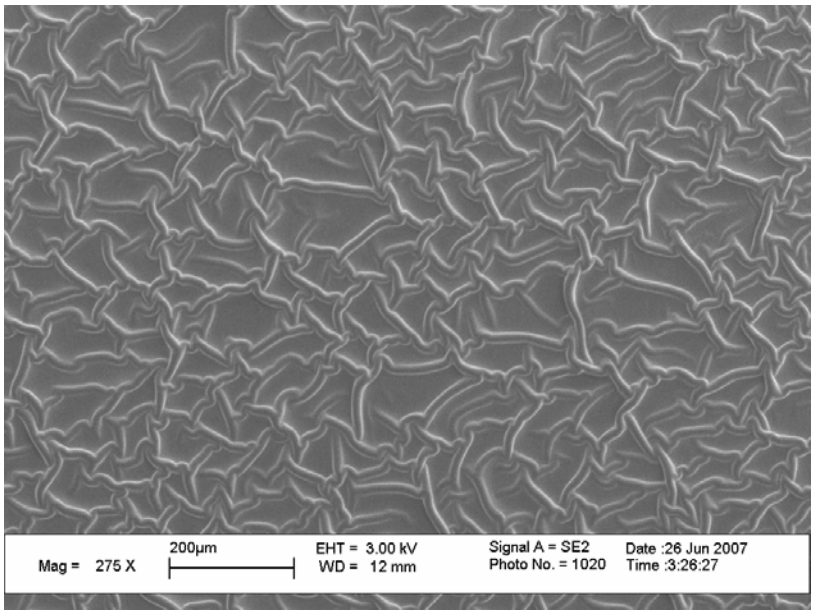

Figure 3-9 SEM image of 10 minute deposited Poly(pyrrole) on ITO electrode (electrode for Type C device)

SEM results of three different electrodes reveals that the long polymerization time could not give rise to more surface area on the electrode, and their surface morphology was almost the same. Therefore it is expected that nearly the same capacitance value in the fabricated supercapacitor by using these electrode materials since the capacitance is directly proportional to the surface area of electrode.

3.2.2 Characterization of polymer electrolyte

The electrolyte is another effective component of an electrochemical capacitor. The voltage applied to an electrochemical capacitor is limited by the electrolyte decomposition voltage. For aqueous electrolytes decomposition value is around 1.0 V, while for organic electrolytes it is around 3 V. Because the energy storage is given by $E= ½ CV^2$, organic electrolytes are attractive for producing a higher energy density electrochemical capacitor than is possible with aqueous electrolytes [44].

Also many redox supercapacitors based on liquid electrolytes have been reported by the scientist, but these are related to well known disadvantages of leakage, corrosion, self discharge, low energy density, and bulky design [45]. That is why realizing of solid-state redox supercapacitors based on conducting polymer electrodes and solid polymer electrolytes has been focused in this study.

The composition of the solid polymer electrolyte should be first optimized in order to obtain substantially conducting, and mechanically stable and flexible material as well as the optimum compositions of the electrolyte chosen for the construction of the redox capacitors. The resulting electrolyte should possess the conductivity of the order of 10^{-3} Scm^{-1} at room temperature with good mechanical strength, flexible enough to mold in the desirable area. This order of conductivity is acceptable for usage in capacitor applications since the electrolyte offer low resistance when used in the film form of thickness 200-300 μm cm^{-2}.

The electrolyte which is utilized to construct the supercapacitors was chosen as PVA-H_3PO_4 as the separator in this project. The separator is placed between the electrodes in order to prevent electrical contact, but it still allows ions to pass through

the electrolyte. The resultant polymer electrolyte has been characterized regarding its thickness and electrical conductivity. The thickness of the proton conducting polymer electrolyte of PVA-H_3PO_4 film has been measured using the Dektak surface profiler. As seen in Figure 3-10, the thickness of the polymer electrolyte has been found approximately 51 μm.

Figure 3-10 Measured result of the PVA-H_3PO_4 thickness

For the measurement of the bulk electrical conductivity of polymer electrolyte film, ac. impedance spectroscopy was utilized. The conductivity of the electrolyte film was found in the order of 10^{-4}-10^{-3} S cm^{-1} for the temperature of 25 C^o. This order of conductivity is acceptable as it gives low resistance when a thin film form of the polymer electrolyte is used in a supercapacitor. For example, for a film of 200 μm thickness and area 4.0 cm^2 with conductivity 10^{-4} S cm^{-1} the resistance would be 50 Ω.

3.2.3 Characterization of fabricated supercapacitors

Generally, three possible configuration types for the redox supercapacitor device, in which the conducting polymers are used, have been projected in the literature. In type-I capacitors, two similar electrodes which are based on p-dopable conducting

polymers are utilized symmetrically, while in type-II capacitors, two different p-dopable conducting polymers are employed. For type-III capacitors, one electrode can have n-dopable; the other one can have p-dopable polymers. In this work, all solid state redox supercapacitors fabricated as in type-I configuration which means two electrodes, which are designed for the supercapacitor, are the same and p-dopable.

Determinations of the double layer capacitance and its potential dependence provide us detailed information for examining the behavior and structure of electrified interfaces. It is mainly because the dependence of the charge, q, held on each side of the electrode interface on the measured electrode potential, E (which is equivalent to the Fermi level of electron energy states in the metal) is directly determinable as a differential quantity, C_{dl}, dq/dE; such types of quantities always give more resolved information than do corresponding integral relations, e.g., total charge q plotted versus the electrode potential E at which it has been accumulated, or q divided by E at a electrode given potential. That is why cyclic voltammetry and ac impedance measurements which both give differential information [46] are especially valuable and preferred in this study.

3.2.3.1 Cyclic voltammetry results

Cyclic voltammetry is a dynamic electrochemical method in which the potential applied to an electrochemical cell is scanned and the resulting cell current is output versus potential, for measuring redox events. It can be used to study the electrochemical behavior of species diffusing to an electrode surface, interfacial phenomena at an electrode surface, and bulk properties of materials in or on electrodes. In addition, providing an estimate of the redox potential it can also give information about the rate of electron transfer kinetics between the electrode and the electrolyte, and as well as the stability of the electrolyte.

Instrumentation for modern cyclic voltammetry is based on the three electrode potentiostat, which controls the potential of the working electrode versus the reference electrode, while compensating for as much of the cell resistance as possible. The

potentiostat and cell design allow events at the working electrode to be monitored during the experiment.

The potential scan is programmed to begin at an initial potential where no electrolysis occurs. The scan continues at the desired linear scan rate to the switching potential, then reverses direction and returns to the initial potential. The output of cyclic voltammetry is a plot of the current flowing in the electrochemical cell due to a redox reaction during the cyclic potential scan.

The achievement of rectangular-shaped cyclic voltammograms in a wide range of scan-rates is the crucial aim for electrochemical capacitors. This performance is required for practical applications because a higher energy density is expected when the utilizable potential range is wide. Furthermore, a higher power density is expected as the critical scan rate increases. The obtained rectangular shaped cyclic voltammograms suggest that the used electrode materials are a brilliant candidate for electrochemical capacitors. Also the obtained information related to increasing current with increasing scan rate by cyclic voltammogram, suggests that there is capacitive nature in electrode material. The linearity of the curve which is occurred by anodic peak current values versus increasing scan rate values means that the process is not diffusion controlled in that scan rate range.

The following figures show cyclic voltammograms of a prepared different type of capacitor cells at a different voltage scan rate.

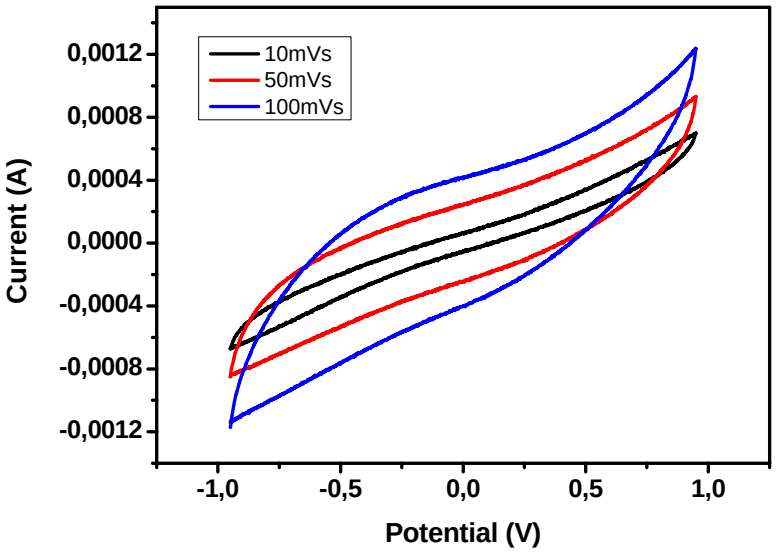

Figure 3-11 Cyclic voltammogram of Type-A supercapacitor at different scan rates: 10, 50, 100 mV/s.

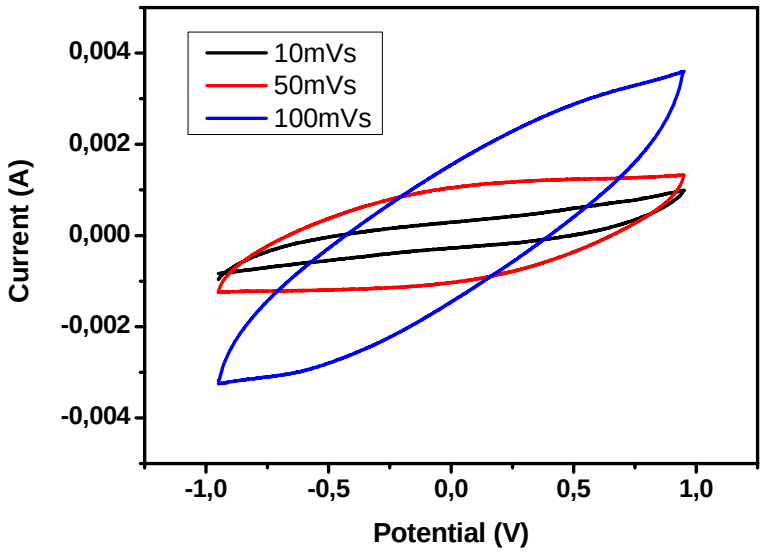

Figure 3-12 Cyclic voltammogram of Type-B supercapacitor at different scan rates: 10, 50, 100 mV/s.

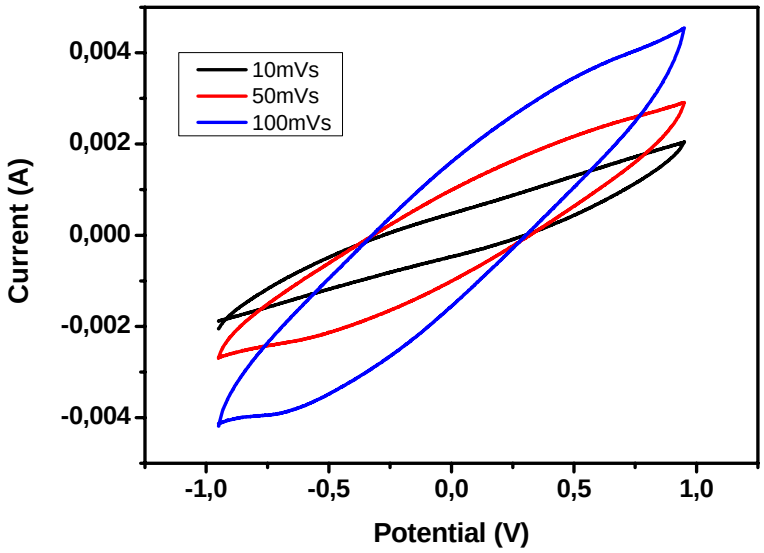

Figure 3-13 Cyclic voltammogram of Type-C supercapacitor at different scan rates: 10, 50, 100 mV/s.

Results from Figure 3-11 to Figure 3-13 show the current versus potential difference curves of the realized capacitor structures. Measurements start with applying -0.95 V potential difference between the electrodes of the capacitor and finalize at the 0.95 V. The applied potential difference range was chosen widely as much as possible, due to the fact that energy density is directly proportional to the voltage. Since the used proton based polymer electrolyte has a decomposition voltage at around 1.0 V, the applied maximum voltage was chosen as 0.95 V.

The cyclic voltammogram response for each fabricated cell has been found to be dependent on scan rate as expected for a capacitor cell. At a low value of scan rates (10-50 mV/s), the cyclic voltammograms show ideal rectangular shape for fabricated capacitor cell. In the case of Type B cell, the best rectangular shape at 10 mV/s and 50 mV/s scan rates was observed.

The electrical behavior of fabricated capacitors is represented as an ideal capacitor connected in series with a resistance (internal resistance) and the circuit has a finite value of RC time constant. The time scale of the measurement approaches the time constant of the circuit; therefore, a deviation of cyclic voltammograms from their rectangular shape has been observed at high scan rates as seen from all cyclic

voltammogram figures. The internal resistance of the fabricated capacitor cells is not low at high scan rates, so there is an obvious deviation from the rectangular shaped cyclic voltammogram which is an ideal characteristic of a real capacitor at these rates.

From these cyclic voltammogram results of fabricated cells, specific capacitance which depends on the total stored charge has been calculated. Capacitance per area (C_S) could be easily calculated by taking the integral over the scan rate of the I-V curve and divided by the total area as in equation (3.1) [6];

$$C_S = \frac{\int i \frac{dt}{dv}}{Total\ Area} \qquad \textbf{(3.1)}$$

The specific capacitance values evaluated from the ratio of the integrated current to the sweep rate for 50 mV/s, are shown in Table 3-1.

Table 3-1 Spesific capacitance of fabricated capacitors evaluated from cyclic voltammogram measurements

Type of Device	**Specific Capacitance**
Type A	6,55 mF/cm^2
Type B	21,55 mF/cm^2
Type C	21,09 mF/cm^2

The results of Table 3-1 reveals that polymerization time on directly ITO substrate increases the device specific capacitance as proved when compared to Type-A, Type-B. However, the increment of the capacitance continued until its saturated state was reached. Additional duration of polymerization after 5 minute could not give rise to more capacitance in the device, as observed from the comparison of Type-B and Type C device.

3.2.3.2 Impedance spectroscopy results

Electrochemical impedance spectroscopy (EIS) is a powerful technique to analyze the capacitive behavior for electrochemical cells. This technique can provide information on electrochemical responses of interfacial structures and processes. For impedance measurements, a sinusoidal signal is applied to the test electrodes and the response is acquired by measuring the magnitude and phase shift of the resulting current.

There are two types of impedance diagrams as a response for the measurements, namely, Nyquist and Bode plots. In a Nyquist plot, the impedance is expressed by a real part Z' and an imaginary part Z'' of the total complex impedance with the equation (3.2),

$$Z = Z'_{real} + jZ''_{imaginary} \qquad \textbf{(3.2)}$$

where $j = \sqrt{-1}$ [47, 48].

In a response by the Bode plot, both the magnitude and phase angle of impedance are plotted as a function of frequency.

The following figures, from Figure 3-14 to Figure 3-16, show the impedance plots (Z_{real} versus $Z_{imaginary}$) of all the fabricated electrochemical capacitor cells. This type of graphs is also called Nyquist plot.

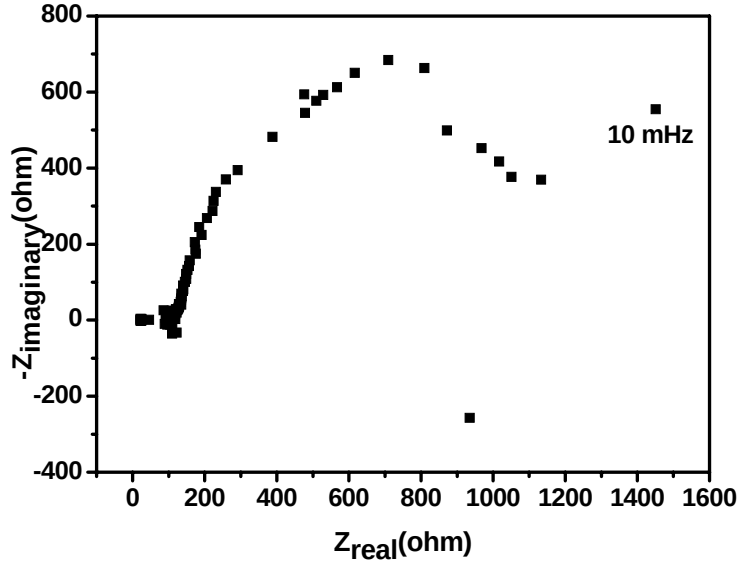

Figure 3-14 Impedance plot of Type A capacitor cell in the frequency range of 10 mHz to 100 kHz.

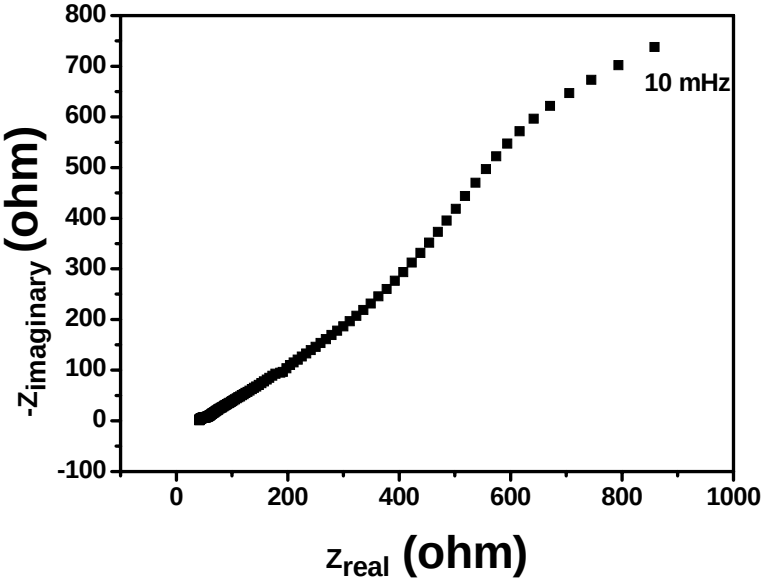

Figure 3-15 Impedance plot of Type B capacitor cell in the frequency range of 10 mHz to 100 kHz.

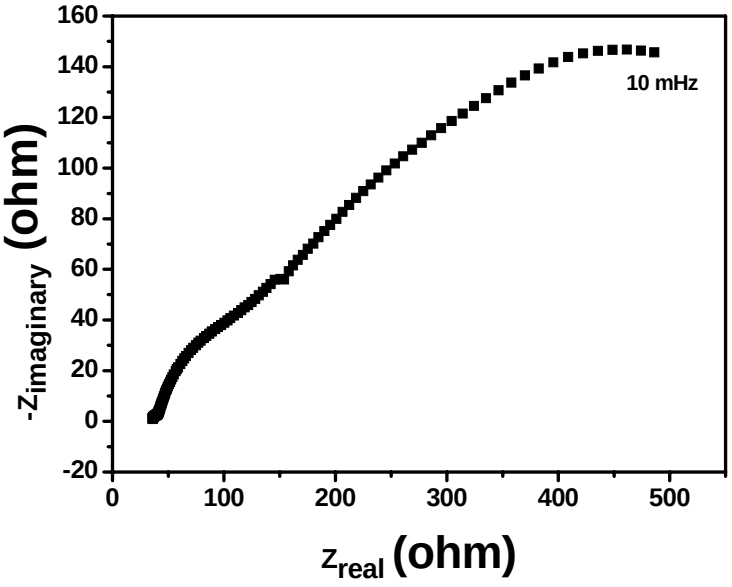

Figure 3-16 Impedance plot of Type C capacitor cell in the frequency range of 10 mHz to 100 kHz.

From the resulting graphs, devices based on poly(pyrrole) show capacitive behavior. In particular, the cells constructed by the deposition of poly(pyrrole) directly on ITO, show an impedance behavior which has a Nyquist plot nearly to an ideal impedance response for a pure capacitor. It should be noticed that a straight line parallel to the imaginary axis is an ideal capacitor behavior for impedance response. From analysis of the figures, it can be said that the more resistive behavior, which comes from Z_{real} value, than capacitive behavior was obtained by decreasing the duration of polymerization on ITO electrodes.

The capacitance values were calculated at the frequency value as low as possible. The frequency of 60 mHz was utilized to calculate the specific capacitance because of electrochemical capacitance at the electrode-electrolyte interfaces (which are several orders larger than the geometrical capacitance) are dominant in the low frequency region [49, 50]. The overall capacitances C of the cells were calculated using the formula in (3.3):

$$C = -(\omega . Z_{im})^{-1} \qquad \textbf{(3.3)}$$

where ω $(=2\pi f)$ is the angular frequency and Z_{im} is the imaginary part of the total complex impedance. Measurement results which include the specific capacitance of fabricated cells at 60 mHz have been given in Table 3-2.

As seen from the Table 3-2, capacitance values of the devices directly proportional to the polymerization time on the electrodes.

Table 3-2 Specific capacitances of fabricated capacitors evaluated from impedance measurements

Type of Device	**Capacitance @ 60 mHz**
Type A	9,60 mF/cm^2
Type B	10,11 mF/cm^2
Type C	31,57 mF/cm^2

Although the measured specific capacitances of the fabricated devices by using ac. electrochemical impedance spectroscopy were completely different from the results obtained cyclic voltammetry, this situation is very typical in the literature as well. The difference is explained as the difference of the measurement potential signal type.

3.3 Conclusions

The preliminary objective of this study was to realize highly-surfaced conductive polymer in nano size for supercapacitor applications. The template synthesis technique was successfully applied to obtain Poly(N-methylpyrrole) nano arrays. Scanning electron microscopy results indicates that it was possible to obtain continuous, homogeny, and well ordered conducting polymer in the nano size with the existence of the surfactant. Additionally, use of template proves that desired conducting polymer structures in nano-scales could be clearly reached. Combining gold nano-particles on the conducting polymer fibers has also been attempted to

improve the electrical conductivity of the material. From the SEM results of this study, gold nano particles were combined with the polymer structure even if they were not directly deposited on the fiber structure. Although the production of conducting polymer in nano-form has been achieved successfully, the material obtained could not be utilized as the active material in fabricated supercapacitor because of the absence of suitable current collector to attach the obtained material to the capacitance measurement devices. Therefore, a different electrode material has been directly produced on the current collector to realize and characterize supercapacitor.

For this alternative electrode material, pyrrole monomer was used and its electrochemical polymerization on ITO realized for a different duration of polymerization. The produced electrodes were completely used for the fabrication of supercapacitors. Their characterization was performed by cyclic voltammeter and ac impedance spectroscopy technique. From the results of cyclic voltammeter measurements, polymerization time on ITO was directly proportional to the capacitance of device until 5 minute. After 5 minute duration of polymerization on ITO electrode, the device has reached its saturated capacitance value which is approximately 21mF/cm^2. On the other hand, the resulting capacitance values at the frequency of 60 mHz by using ac. electrochemical impedance spectroscopy indicated that the capacitance values are directly proportional with the polymerization time on electrode materials. However, the capacitance values differ when compared the results obtained from cyclic voltammetry measurement that is typical for this method, because of the hindrance of the alternative current's penetration into pores of electrode materials.

REFERENCES

[1] W. Z. L. J.H. Chen, D.Z. Wang, S.X. Yang, J.G. Wen, Z.F. Ren, *Carbon* vol. 40, pp. 1193–1197, 2002.

[2] F. D. Farmer JC, Mack GV, Pekala RW, Poco JF. J, *Electrochem Soc* vol. 143, pp. 159, 1996.

[3] C. BE, *J Electrochem Soc* vol. 138, pp. 1539, 1991.

[4] J. A. I. Bispo-Fonseca, C. Sarrazin, P. Simon, J.F. Fauvarque, *Journal of Power Sources* vol. 79, pp. 238–241, 1999.

[5] A. Burke, *J. Power Sources*, vol. 91, pp. 37., 2000.

[6] P. L. T. C. Portet, P. Simon, E. Flahaut, C. Laberty-Robert, *Electrochimica Acta* vol. 50, pp. 4174–4181, 2005.

[7] Y. I. Y. Takamuku, J. Ozaki, *International Conference on Advanced Capacitors*, 2003.

[8] M. M. C. Arbizzani, L. Meneghello, R. Paraventi, *Adv. Mater.* , vol. 8, pp. 331, 1996.

[9] A. L. Aurelien Du Pasquier, Patrice Simon, Glenn G. Amatucci, Jean-Francois Fauvarqueb, *Journal of The Electrochemical Society*, vol. 149, pp. A302-A306, 2002.

[10] D. J. Dominique Villers, Chantal Soucy, Daniel Cossement, Richard Chahine, Livain Breau, Daniel Be´langera, *Journal of The Electrochemical Society*, vol. 150, pp. A747-A752, 2003.

[11] A. J. Heeger, "Semiconducting and metallic polymers," *Angew. Chem. Int. Ed.*, vol. 40 pp. 2591–2611, 2001.

[12] J. H. O. J. Jang, G.D. Stucky, "Fabrication of ultrafine conducting polymer and graphite nanoparticles," *Angew. Chem. Int. Ed.*, vol. 41, pp. 4016–4019, 2002.

[13] A. Burke, *J. Power Sources*, vol. 91, pp. 37–50, 2000.

[14] S. G. Paul M. Fishbane, Stephen T. Thornton, *Physics for scientists and engineers*, 2nd ed. ed. Upper Saddle River, N.J.: Prentice Hall, 1996.

[15] J. A. I. Bispo-Fonseca), C. Sarrazin, P. Simon, J.F. Fauvarque.

[16] E. F. Cathie Vix-Guterl, KrzysztofJurewicz, Marcin Friebe, Julien Parmentier, Franc¸ois Be´guin, *Carbon* vol. 43, pp. 1293–1302, 2005.

[17] K.-B. K. Kyung-Wan Nam, *Journal of The Electrochemical Society*, vol. 149 pp. A346-A354, 2002.

[18] X. Z. Qiangfeng Xiao, *Electrochimica Acta* vol. 48, pp. 575-580, 2003.

[19] F. B. g. E. Frackowiak, *Carbon*, vol. 39, pp. 937, 2001.

[20] D. Qu, *J. Power Sources*, vol. 109, pp. 403, 2002.

[21] B. E. Conway, *Electrochemical supercapacitors : scientific fundamentals and technological applications* New York: Plenum Press, 1999.

[22] A. S. w. S. Biniak, M. Pakuła, "Chemistry and Physics of Carbon," vol. 27, pp. 125, 2001.

[23] M. M. C. Arbizzani, L. Meneghello, *Electrochim. Acta* vol. 41, pp. 21, 1996.

[24] H. S. Malcolm D. Ingrama, Karl S. Ryder, *Solid State Ionics* vol. 169, pp. 51–57, 2004.

[25] P. S. F. Lufrano, M. Minutoli, *Journal of The Electrochemical Society*, vol. 151, pp. A64-A68, 2004.

[26] J. M. Li-Zhen Fan, *Electrochemistry Communications* vol. 8, pp. 937–940, 2006.

[27] A. G. A. Di Fabio, M. Mastragostino, F. Soavi, *Journal of The Electrochemical Society*, vol. 148, pp. A845-A850, 2001.
[28] P. S. A. Laforgue, J. F. Fauvarque, M. Mastragostino, F. Soavi, J. F. Sarrau, P. Lailler, M. Conte, E. Rossi, S. Saguattie, *Journal of The Electrochemical Society*, vol. 150, pp. A645-A651, 2003.
[29] P. S. A. Laforgue, J. F. Fauvarque, M. Mastragostino, F. Soavi, J. F. Sarrau, P. Lailler, M. Conte, E. Rossi, S. Saguattie, *Journal of The Electrochemical Society*, vol. 150, pp. A645-A651, 2003.
[30] C. Jung Yong KimIn Jae, *Journal of The Electrochemical Society*, vol. 149, pp. A1376-A1380, 2002.
[31] C. K. a. K. S. Yang, *Applied Physics Letter*, vol. 83.
[32] V. K. K. Lotaa, E. Frackowiak, *Journal of Physics and Chemistry of Solids* vol. 65, pp. 295–301, 2004.
[33] C. A. M. Mastragostino, R. Paraventi, A. Zanellia, *Journal of The Electrochemical Society*, vol. 147, pp. 407-412, 2000.
[34] R. J. L. S. A. Hashmi, R. G. Linford, W. S. Schlindwein, *J. Chem. Soc. Faraday Trans.*, vol. 93, pp. 4177, 1997.
[35] M. A. A. S.H. Pang, T.W. Chapman, *J. Electrochem. Soc.*, vol. 147, pp. 444–450, 2000.
[36] D. A. E. Q.L. Fary, S.L. Robertson, J.P. Zeng, *J. Electrochem. Soc.*, vol. 148, pp. A833–A837, 2001.
[37] P. L. T. J. Gamby, P. Simon, J.F. Fauvarque, M. Chesneau, *J. Power Sources* vol. 101, pp. 109–116, 2001.
[38] K. H. T. Morimoto, Y. Sanada, K. Kurihara, *J. Power Sources*, vol. 60, pp. 239–247, 1996.
[39] I. P. A. Du Pasquier, S. Menocal, G. Amatucci, *J. Power Sources*, vol. 115, pp. 171–178, 2003.
[40] P. S. A. Laforgue, J.F. Fauvarque, M. Mastragostino, F. Soavi, J.F. Sarrau, P. Lailler, M. Conte, E. Rossi, S. Saguatti, *J. Electrochem. Soc.*, vol. 150, pp. A645–A651, 2003.
[41] H. S. M.D. Ingram, K.S. Ryder, *Solid State Ionics*, vol. 169, pp. 51, 2004.
[42] A. E. P. D.T. McQude, T.M. Swager, "Conjugated polymer-based chemical sensors," *Chem. Rev.* , vol. 100, pp. 2537–2574, 2000.
[43] M. A. K. D.B. Cairns, C. Perruchot, A. Riede, S.P. Armes, "Synthesis and characterization of polypyrrole-coated poly(alkyl methacrylate) latex particles," *Chem. Mater*, vol. 15, pp. 233–239, 2003.
[44] H. A. H. Patrick Soudan, Livain Breau, Daniel Belangera, *Journal of The Electrochemical Society*, vol. 148, pp. A775-A782, 2001.
[45] P. G. Florence Fusalba, Dominique Villers, Daniel Bélanger, *Journal of The Electrochemical Society*, vol. 148, pp. A1-A6, 2001.
[46] P. S. P. L. Taberna, J. F. Fauvarque, *Journal of The Electrochemical Society*, vol. 150, pp. A292-A300, 2003.
[47] P. L. T. C. Portet, P. Simon, E. Flahaut, *Journal of Power Sources* vol. 139 pp. 371–378, 2005.
[48] I.-H. Y. Jong-in Hong, Woon-kie Paika, *Journal of The Electrochemical Society*, vol. 148 pp. A156-A163, 2001.
[49] T.-C. W. W.-C. Chen, H. Teng, *Electrochim. Acta*, vol. 48, pp. 641, 2003.
[50] R. D. Levie, *Electrochim. Acta*, vol. 8, pp. 751, 1963.